May 2013

Voltage Stability Assessment Using P-Q Region Incorporating Wind Power

You Wang
University of Wisconsin-Milwaukee

VOLTAGE STABILITY ASSESSMENT USING P-Q REGION INCORPORATING WIND POWER

by

You Wang

A Thesis Submitted in

Partial Fulfillment of the

Requirements for the Degree of

Master of Science

in Engineering

at

The University of Wisconsin-Milwaukee

May 2013

ABSTRACT
VOLTAGE STABILITY ASSESSMENT USING P-Q REGION INCORPORATING WIND POWER

by

You Wang

The University of Wisconsin-Milwaukee, 2013
Under the Supervision of Professor David C. Yu

Voltage stability assessment (VSA) is a significant part in planning and operating of the power system. As one of the classic static VSA method, the P-V curve is widely used in identifying the weak buses in one power system. Normally, there is a required range of bus voltage variation that restricts load with fixed power factor within a maximum value. The loading margin can be defined as the distance between the operating point and the maximum load. The proposed P-Q region, which defines safe region for voltage stability, is more effective and intuitional when applying to VSA compared to the P-V curve. However, it is necessary to verify the feasibility of the novel method before implementing this method in system incorporating wind power penetration. Simulations using MATPOWER and contrastive calculating results prove the accuracy of P-Q region. Also, the calculation method of the

probability of output power of the wind farm is proposed. In this approach, the P-Q regions at different levels of wind power penetration are presented and discussed. Moreover, the P-Q region is proposed as a tool to determine the best location to place a wind farm as well as assess the safe operating zone of the reactive power with respect of the variable real power output. Finally, the expected loading margin validates the effectiveness of the proposed P-Q region method and its applications when incorporating wind power.

TABLE OF CONTENTS

LIST OF FIGURES

LIST OF TABLES

ACKNOWLEDGEMENTS

I wish to thank various people for their unselfish help and priceless support during the whole process of accomplishing this dissertation.

Firstly, I would like to express my deepest gratitude to my major advisor, Professor David C. Yu, for helping me come up with the meaningful topic, as well as his patient guidance, enthusiastic encouragement, and useful critiques for my research work. Especially, I am so grateful that Professor Yu devotes himself to building up the communicational bridge between the universities in China and the University of Wisconsin-Milwaukee, which gave more opportunities to many college students like me to come to United States for further study and a better educational environment. Also, I would like to thank him for offering me the lab assistantship that alleviated the economic pressure and helped me concentrate on my thesis.

Besides my advisor, my sincere thanks also go to my teammates Qiang Fu and Lei Yu for their time for discussions and their valuable suggestions over the duration of my research.

I would also extend my thanks to the University of Wisconsin-Milwaukee for providing me the precious opportunity, scholarship and abundant academic resources. I have to show deep appreciation to those

patient and friendly staff for their kind help and guidance during this one-year study.

Last but never the least, thanks to my parents Yong Wang and Xiaoying Tang for creating my life and giving me their unselfish love. I would never have this change to study abroad without their sacrificial support. Thanks to my fiancé Xi Chen, for offering the positive strength and encouragement all the time.

CHAPTER 1 INTRODUCTION

1.1 Motivation

With the development of modern power systems, fast-growing load demand, long-distance transmission lines and increasing implication of multiple power electronic elements have led to a more stressed system than ever before. As an indispensable role in human life and all aspects of society, the power grid is aimed at providing electricity economically, safely, and stably. However, due to the intricacy and indeterminacy of this tremendous network, meeting these goals when operating an actual system is never as facile as it seems to be.

Since 1920's, the reliability and stability analysis has been realized as a significant part of analysis of power system. Research in this field focuses on three aspects: angle stability, voltage stability and frequency stability. Less attention was paid to voltage stability than to angle and frequency's stability until 1970's when a series of outage and blackout faults caused by voltage collapse happened worldwide and highlighted the severity of voltage instability. Carson Taylor reported several severe voltage collapse incidents in recent decades (see Table 1) [1]

Table 1 Voltage Collapse Incidents

Date	Location	Time Frame
11/30/86	SE Brazil, Paraguay	2 Seconds
5/17/85	South Florida	4 Seconds
8/22/87	Western Tennessee	10 Seconds
12/27/83	Sweden	50 Seconds
9/22/77	Jacksonville, Florida	Few minutes
11/26/82	Florida	1-3 Minutes
12/28/82	Florida	1-3 Minutes
12/30/82	Florida	1-3 Minutes
12/09/65	Brittany, France	?
11/20/76	Brittany, France	?
8/04/82	Belgium	4.5 Minutes
1/12/87	Western France	4-6 Minutes
7/23/87	Tokyo	20 Minutes
12/19/78	France	26 Minutes

The direct economic loss and indirect effects on the power-related industry are enormous. The famous “8.14” large scale blackout incident in eastern America and Canada caused black out spreading across eight states of US and two provinces of Canada. The area of outage was up to 9300 km^2, the estimated direct economic losses were more than 35 billion dollars, and the population affected by this accident was more than 50 million people [2] The post-accident surveys point out that all these voltage collapse incidents happened all of a sudden and are difficult to detect before the advent of fast and wide-range voltage decline. The voltage collapse incidents are found to

be an irreversible and fast-moving episode progress that happens when the power system is changed slowly by the adjustment of the control devices such as LTC or Statcom after large disturbance. That is the reason why it is difficult for operators to take emergency measures before the failure happens. All these reasons motivate researchers to pay attention to how to prioritize the voltage stability assessment.

1.2 Research Status

1.2.1 Definition and Classification of Voltage Stability

Kundur in his book mentioned that the collapse of load voltage is a kind of instability encountered without loss of synchronism [3]. A generally accepted concept is defined by the IEEE/CIGRE joint task force [4] as the ability of a power system to maintain steady voltages at all buses after the system is subjected to a disturbance from a given initial operating condition.

The task force further classified the voltage stability into four categories:

Large-disturbance voltage stability: the ability to maintain stability after suffering large disturbances like systematic faults, generation faults or trapped transmission lines. The objective period of study maybe a few seconds or several minutes.

Small-disturbance voltage stability: the ability to maintain steady voltages when subjected to small perturbations such as incremental changes in system load. This form of stability is influenced by the characteristics of loads, continuous controls, and discrete controls at a given time instant.

Short-term voltage stability: involves dynamics of fast acting load components such as induction motors, electronically controlled loads and converters. The study period of interest is in the order of several seconds, and analysis requires solution of appropriate system differential equations.

Long-term voltage stability: involves slower acting equipment such as tap-changing transformers, thermostatically controlled loads and generating current limiters. The study period of interest may extend to several or many minutes, and long-term simulations are required for analysis of system dynamic performance.

1.2.2 Mechanism of Instability

In order to come up with the methods to assess voltage stability, the very first step is figuring out how and why the system loses control. Understanding the physical essence of voltage instability development is the cornerstone of voltage stability research.

Voltage instability, which started with progressive degradation of the bus voltage profile, is generally considered to occur when the system suffers

from severe contingencies or lacks reactive power supply during the load pick-up period. There are diverse voices on the explanation of voltage instability. One popular idea is that the loss of voltage stability is contributed by joint effect of the load variation properties and on-load tap changing transformer (OLTC)， as well as generator overexcited limit (OEL). The system bus voltage can maintain an accepted level by reducing the load owing the forced exciting regulation of generators and voltage sensitivity of load. In the meantime, progressive restored load due to the regulation of OLTC leads to overstepped exciting field current in generators. The chain response of these factors causes the irreversible load voltage degradation. In other words, voltage instability is caused by the already stressed system trying to operate beyond the maximum transmission power.

1.2.3 Main Methods of Voltage Stability Assessment

Voltage Stability Assessment (VSA) aims at obtaining any kinds of criteria for power system planning or operating to be aware of the margin between the operating points and critical situations, as well as the probability of the voltage collapse in various contingencies. Based on different considerations over various contingencies, multiple methods are discussed and developed in order to be qualified in different utilities. Among all the factors, accuracy, efficiency and economy are of utmost concern. Generally

speaking, the research approaches can be divided into two categories: static analysis and dynamic analysis.

In terms of the essence of voltage stability, dynamic analysis can provide more accurate references for the assessment. That is because the generators, as well as their exciting control system, OLTC, reactive compensation equipment etc. and load dynamic properties all have significant influence on voltage stability. Dynamic analysis, which counts for those influences, can give precise reflection of the status of system voltage stability [5] Therefore, dynamic analysis can be helpful in situations when the system suffers from large disturbance such as loss of main generators, tripping of transmission lines, or two connected systems becoming separated because of the system faults. One assignable shortcoming of dynamic analysis is that it is incapable of providing the sensitivity or degree of stability. What's more, the progress computation is extremely time-consuming because this analysis is based on the differential and algebraic equations used to describe this phenomenon [6].

Static analysis is more practical considering its efficiency and accuracy in most cases in which the system dynamics have very slow influence on voltage stability. Static approaches examine the feasibility of

fixed operating point by several indices that can provide system operators the voltage stability margins in order to indicate the sensitivity of stability.

Basically, static analysis is established on power flow equations. So the stability problem can be regarded as whether the power flow equations have keys. In this way, every critical key corresponds to one voltage stability limit point. Deficiency of reactive power supply is considered to be the direct reason of voltage degradation, so the main interest of voltage stability analysis lies in power transfer margin determined by both the system and the load condition. The well-known P-V curve and Q-V curve are commonly used to determine the permissible loading within the voltage stability limit [7]-[8]. There are other methods, such as multiple developed load flow solutions [9] and singularity judgment of the Jacobian matrix [10]. The P-V curve can give operators a more intuitive and visual way to determine how close the operating point is to the limit and predict the maximum loading. Although QV curves offer the measurement of reactive power margin to instability point, they often fail to identify the true weak points as addressed in [11] and [12]. P-V curves directly reveal the relationship between the real power load and the bus voltage. The “nose” point stands for the voltage collapse point. P-V curves can be used either in planning or in operating. It’s

highly requisite to profoundly discuss such a useful method and analyze all of its properties in order to conclude the effect of wind penetration.

Haque [13] raised a new method for VSA by using the P-Q curve. This idea was inspired by the established basic concept that voltage instability happens when the system is trying to transfer power beyond its limitations. Once the margins of P and Q are determined, the voltage stability can be directly assessed. The mechanism of P-Q curves will be introduced in Chapter 2 in detail.

1.3 The effect of wind penetration

As energy-related pollution increased worldwide, the related environmental problems have received much more attention than ever before. Even if the fossil fuels are still occupying a significant part of the energy supply of modern power systems, the development of renewable energy has begun its rapid growth. Solar, nuclear and wind power are the most promising potential energies of all the proposed possible energy forms. The biggest problem for solar energy is the huge cost of storage battery; meanwhile low efficiency is also an obstacle that prevents it from being the main power supply for power system. It is well known that the nuclear energy station has strict conditions of location, which means it cannot be applied generally. Nowadays the relatively mature application technology

makes wind power the most competitive and efficient renewable energy, and as a result, its portion utilized in renewable energy has a significant and continuous increase. However, with increasing penetration of wind power to the power system, the effect on all aspects of the system starts to emerge due to the randomness of wind and the special generator utilized in the wind power technology. Those effects may cause potential serious problems because the original security margin assessment of the system has been changed obviously while the operating method hasn't been adjusted properly.

Based on the consideration of wind power properties, the doubly fed induction generators (DFIG) are installed as a proper method to manipulate the intermittent and variable wind power. In contrast to conventional synchronous generators, DFIGs have different method of operating the reactive power. It is demonstrated in some literature that the reactive power complement capacitor installed in the DFIG parks can also be an important factor to the power system voltage stability assessment.

Increasing research on the influence of high penetration of wind power to the power system is focused on several issues related to security, stability, power quality and operation of power systems [14]. Power flow can be significantly affected by the stochastic wind power supply as well as

the special properties of DFIG. The injection of real power by wind turbine can meanwhile cause the reactive power loss.

- Voltage stability is of critical concern both in its frequency and magnitude. Incorporation of wind energy may lead to the change of voltage profile.
- Power electronics equipped with wind farm to improve the voltage quality can cause harmonic distortion problems.
- The altered power flow will affect the former protection system, which may fail to be activated when fault happens.

1.4 Textural Work

This dissertation focuses on the voltage stability assessment. Chapter 2 introduces the basic concept of the P-V curve and the P-Q region, and it also gives the pseudo codes of plotting the P-V curve and the P-Q region under the circumstance of MATLAB. In chapter 3, the loading margins calculated from the P-Q regions will be compared to those got by using the classic P-V curves. Based on the study of P-Q region, in the chapter 4 using the P-Q region to determine the best location to place the wind farm will be discussed. Combining with the probabilities of wind power output, the expected loading margins to avoid the voltage violation are estimated under

different levels of wind power penetration utilizing the power flow computation tool MATPOWER.

CHAPTER 2 METHODOLOGY

Voltage instability typically happens when the system is over loaded, faulted or short of reactive power supply. So the most interest lies on the relationships between real power transferred to the load (P), receiving end voltage (V) and reactive power injection (Q). In this chapter, the fundamental concepts of the P-V curve and the P-Q region and how the P-V curve and the P-Q region used as tools of voltage stability assessment will be introduced.

2.1 Synopsis of P-V curve and P-Q region

P-V curve: One important cause of voltage instability is the system has difficulty in meeting the demand of reactive power. This can be explained as the real and reactive power transfer through the inductive reactance representing the transmission network the voltage may drop significant value due to the reactive power loss. The more the power transferring on the line, the more the voltage magnitude may drop. Essentially speaking, voltage instability is a local phenomenon. The way to investigate it should be focus on each bus.

Beyond any doubt, accompanied by increasing P load, Q consuming will also get bigger no matter which kind of load it is. Thus, the relationship

of P (real power load demand) and V (the receiving end voltage magnitude) is of great interest. This non-linear relationship could be studied in a simple two-end radial system showing in figure. Assuming the voltage source $\widetilde{E_s}$is constant which can provide infinite power. The load $\tilde{Z}_{load}$ is supplied through simplified transmission line represented by $\tilde{Z}_{line}$. If the angles of load impedance and line impedance are φ , θ respectively, the current magnitude can be expressed as follows

$$I = \frac{E_s}{\sqrt{(Z_{line}cos\theta + Z_{load}cos\varphi)^2 + (Z_{line}sin\theta + Z_{load}sin\varphi)^2}}$$

To simplify as

$$I = \frac{1}{\sqrt{F}}\frac{E_s}{Z_{line}}$$

where,

$$F = 1 + (\frac{Z_{load}}{Z_{line}})^2 + 2(\frac{Z_{load}}{Z_{line}})\cos(\theta - \varphi)$$

The magnitude of ending bus voltage is

$$V = \frac{1}{\sqrt{F}}\frac{Z_{load}}{Z_{line}}E_s$$

The real power received by the load is

$$P = \frac{Z_{load}}{F}(\frac{E_s}{Z_{line}})^2 cos\varphi$$

Initially, as the load demand Z_{load} is relatively higher than Z_{line}, which results in fast increase in I but slow drop in V. This gives increase of P rapidly when Z_{load} decreasing standing for increasing loads demand. After the loads demand beyond a certain value, the P fails to increase anymore although the V keeps declining. This is due to the less value the Z_{load} compared to Z_{line}, so the decrease in V dominates over the increase in I, then P keeps dropping as a net consequence.

Based on the analysis above, we can roughly get the non-linear relationship between P and V as shown in figure 1. The nose point as known as the voltage collapse point because beyond this point the power flow fails to converge, which is indicative of instability. Operation at or near this limit may cause the system face the risks of a large-scale blackout. The x-label parallel line across the limit point divides the curve into two regions: the upper region is viewed as the stable operating zone, in which the power flow has two distinct solutions for each fixed P value; the unstable region below this line contains the physical meaning that the voltage violation cannot be relieved by either shedding load or enhancing the reactive power injection, in other words, an irreversible voltage collapse happened. The so-called saddle bifurcation node [15] corresponds to the maximum P when the power flow fails to converge.

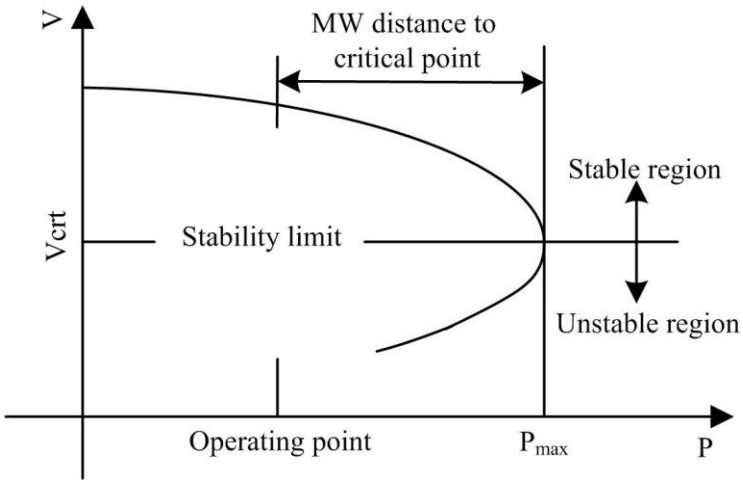

Figure 1. Sketch Map for P-V Curve

Conventionally, the specific buses chosen to be monitored as the load on those buses increasing in order to get the P-V curves on each bus. Note that each P-V curve corresponds to a fixed load power factor. For various power factors, a family of P-V curves can be drawn and they can be used to represent for different types of load.

P-Q region: It's an established fact that the voltage collapse when the system loads (P or Q) increase beyond a certain limit. If the limits of the P and Q are known, the voltage stability margin for a giving operating point can be determined. This requires plotting the voltage stability boundary in P-Q plane. At a certain critical voltage value, with the increasing real power, the reactive power is limited to a certain value in order to meet the requirement of voltage. Then the plotting of the P-Q relationship can decide

a region, inside of which the operation points won't run a risk of voltage collapse.

According to [16], for a specific p, a quadratic equation can be obtained:

$$q^2 + 2{v_{cr}}^2 xq + p^2 - 2v_{cr}^2 rp + v_{cr}^4 - {v_{cr}}^2 = 0$$

Two solution of q are easily got as:

$$q_{lower} = v_{cr}x - \sqrt{-p^2 + 2v_{cr}p + v_{cr}^2 - v_{cr}^4 r^2}$$

$$q_{upper} = v_{cr}x + \sqrt{-p^2 + 2v_{cr}p + v_{cr}^2 - v_{cr}^4 r^2}$$

The lower part of the p-q curve is associated with the consumed power, if the reactive power is treated as a negative value in power flow equation. Based on this formula, the shape of P-Q region can be predicted as a parabola.

The P-Q region, which is restricted by a quadratic curve, stands for the maximum reactive power the system can convey on one certain bus as the real power load increasing. Considering such a basic concept of the P-Q region, it's easy to think of choosing the PV bus to get the P-Q region because the voltage magnitude is constant on those buses. Obviously, one curve is drawn when a certain value of bus voltage magnitude has been set. In other words, under different bus voltages the P-Q regions have different shapes. The most interesting extensions for control center operators are

power margins (measured in MVA, MW and MVAR). P-Q region can simply represent these margins [17], shown in Figure 2. Two sets of margins are presented: loading margins, inherent of the concept of voltage stability probability, where the reactive load margin, $\Delta Q_{loading}$, is of most interest. The active power load margin is denoted as $\Delta P_{loading}$. Another set of reactive power margins, Q-margin, represented as ΔQ. It is known to the concept of Q-V analysis.

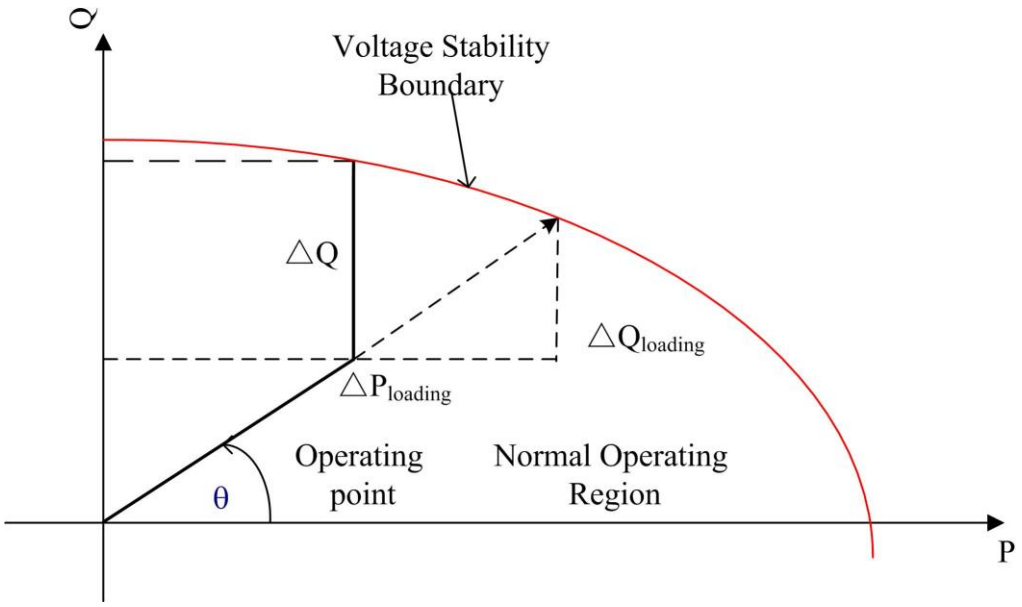

Figure 2. Assessment of Voltage Stability Power Margin

2.2 VSA without Wind Penetration

As mentioned above, solving series of power flow with generally increasing load of fixed power factor each step can generate P-V curve. The main interest of P-V curve is to get the MW margin with respect to the

voltage collapse point or the designated requirement of bus voltage magnitude. From this point of view, the unstable region is of less interest so that we don't need to consider continuous power flow solution. MATPOWER is a suitable tool to finish our target. MATPOWER is a package of MATLAB M-files for solving power flow and optimal power flow problems. It is intended as a simulation tool for researchers and educators that is easy to use and modify.

P-V curve: The PQ buses that have higher risk of voltage instability are chosen as the candidate buses of the test system. After this, the methodology of VSA utilizing the generated P-V curve of each load bus can be described as the following pseudo code.

1) Initialize P=0; pf=power factor input by users; bus no.=bus number input by the users;
2) Load case30 to mpc file;
3) Read P load on candidate bus to Po;
4) Modify P load of the candidate bus to P;
5) Modify Q load of the candidate bus to $\frac{\sqrt{1-pf^2}}{pf} * P$;
6) Run power flow and save the results in temp;
7) Read bus voltage from temp to vector variable V;
8) P+1;

9) Iterate step 4) to 8) until the power flow doesn't converge any more; P=P-1;

10) Decrease the increment of P to 0.1; P=P+0.1;

11) Iterate step 8;

12) Plot the P-V curve using V corresponding P;

13) Compute P margin, $\Delta P = P - Po$;

14) End

Translating the pseudo codes into MATLAB language, it's easy to plot the P-V curve of each candidate bus and get their real power margins. To find out the weakest bus of the system, just put all the P-V curves into one diagram using some special orders.

P-Q region: For the P-Q region, not only the PQ buses are considered, but also the analysis of PV buses is included. The basic idea of forming the P-Q region is that for different values of P load, specific Q injection or absorption is matched in order to keep a certain level of bus voltage. For PV buses, the procedure to realize the function of obtaining the P-Q curve is pretty straight forward, because the voltage is constraint to a certain value. So the main interest lies on how to get the Q value against the increasing demand of P. It is quite important to make clear the concept of Q value: it

represents the reactive power the bus needs to generate to or absorb from the entire system.

However, when dealing with the problem of PQ buses, it seems more confused to figure out the Q value since the bus doesn't have the ability to generate any reactive power. Applying the idea mentioned above, we need to figure out every Q value corresponding to each P point. It seems to be feasible, however, to figure out one value of Q, which can meet the critical voltage, a mass of iterations have to be done. For example, if it needs 200 iterations to figure out one specific Q value corresponding to one P value, for 200 distinct P values, 40000 iterations need to be done. What's worse, the simulation step has to be relatively small considering getting a relative precise range or single value of Q. If we view the problem from a sight of energy, things may get easier. Thus, treat the PQ buses as the PV buses. Now that our goal is to plotting the relationship between P and Q on condition of one certain critical voltage, the method of plotting P-Q region for PV buses can be adopted. The little trick is by giving an "imaginary" generator on the target PQ bus without generating any real power, the "generated" reactive power is thus the Q value. The following pseudo codes explain the procedure to form the P-Q region.

1) Initialize P=0; bus no.=bus number input by the users; Voltage=critical bus voltage input by the users;
2) Load case30 to mpc file;
3) Read P load on candidate bus to Po; Read Q load on candidate bus to Qo;
4) If the bus is PQ bus, modify the bus type to PV bus;
5) Add a generator to the modified bus to the generator matrix;
6) Else, find out the number in generator matrix of the corresponding bus;
7) Modify P load of the candidate bus to P;
8) Modify Q load of the candidate bus to 0;
9) Run power flow and save the results in temp;
10) Read bus voltage from temp to vector variable V;
11) Read Q value from the generator matrix of temp to vector variable Q;
12) P+1;
13) Iterate step 7) to 12 until P reaches the expected maximum value.
14) Plot the P-Q curve using Q corresponding P;

15) Compute P,Q margin: draw a line from origin through the operating point, find out the intersection point with P-Q boundary (Pm, Qm) ; $\Delta P = P_m - Po$; $\Delta Q = Q_m - Qo$;

16) End

P-Q region can also be used to identify the weakest bus, which should be coincident with the result got in P-V curves. For different critical voltage values, P-Q regions vary somehow. The relationship between P-V curves and P-Q regions will be demonstrated in chapter 3.

2.3 Calculation of Probabilities of Wind Power

How to quantify the probability of wind power output of a wind turbine is quite important before assessing voltage margin incorporating wind power. Sequential Monte Carlo methods, time-domain simulations are both commonly utilized in such studies. While without the preserve chronological data, these methods are not available. What's more, they are quite time consuming. [18] proposes a framework to determine the characteristics between the probabilities against the output power of wind farm. It's briefly address as follows.

The critical procedure is to propagate wind-speed pdf (probability density function) to the output power uncertainty. As long as we get to know the wind-speed pdf as well as the relationship between output power and the

wind speed, the probability of wind power can be calculated utilizing the random-variable transformation methods.

Wind-speed pdf $f(v)$, is considered to obey the Weibull distribution

$$f(v;k,\lambda) = \frac{k}{\lambda}(\frac{v}{\lambda})^{k-1}\exp-\left(\frac{v}{\lambda}\right)^{k} \qquad v \geq 0$$

, where $k > 0$ is the shape parameter of this function, $\lambda > 0$ is called the scale parameter, v is the wind speed that can't be negative.

The output power function of wind speed, is described as a piecewise continuous function as shown below

$$p(v) = \begin{cases} p_1 = P_r - P_r\left[1 + \exp\left(\frac{v - v_{mid}}{c}\right)\right]^{-1} & ,0 \leq v \leq v_{lim} \\ p_2 = P_r - P_r\alpha(v - v_{mid})^q & ,v_{lim} \leq v \leq v_f \end{cases}$$

, where the parameter v_{mid} denotes the wind speed when the output wind power is half of the rated value; to ensure the p_1 is close enough to the rated power when the wind speed is at the rated speed value, c can be get through the requirement equation, $p_1(v_r) = 0.99P_r$, then $c = (v_r - v_{mid})[\log(\frac{0.99}{1-0.99})]^{-1}$; finally, $a = (v_f - v_{lim})^{-q}$ is got by the constraint condition that $p_2(v_f) = 0$.

Figure 3 is the p-v function of Vestas V90-2.0 MW wind turbine [19] . All the relevant model parameters are illustrated in Table 2.

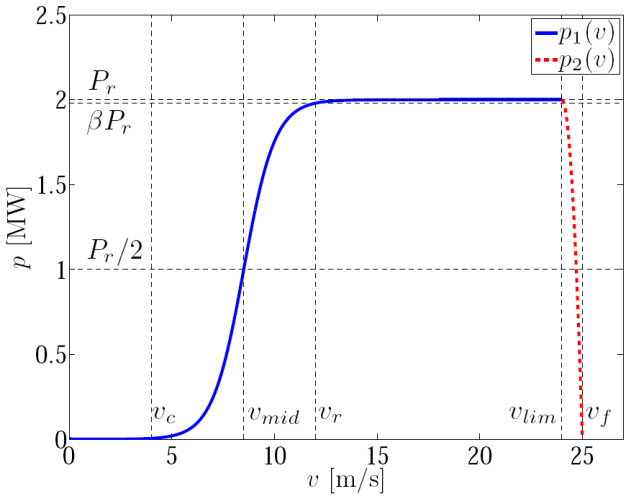

Figure 3. Example $p - v$ Function

Table 2. Wind Turbine Parameters

Symbol	Parameter	Value
P_r	Rated power	2 MW
v_c	Cut-in wind speed	4 m/s
v_r	Rated wind speed	12m/s
v_{lim}	Limiting wind speed	24m/s
v_f	Furling wind speed	25m/s
c	Shape parameter that ensures $p_1(v_r) \approx P_r$	0.7617m/s
v_{mid}	Wind speed such that $p(v_{mid}) = P_r/2$	8.5m/s
q	Order of drop off for $v > v_{lim}$	2
α	Parameter that ensures $p(v_f) = 0$	$1(m/s)^{-2}$

The final step is to propagate wind-speed pdf to probability vs. output power function. Applying random-variable transformations， the random variable v, which stands for the wind speed, with pdf $f(v)$, combining with the p-v characteristics deduces the equation

$$f_p(p) = \frac{f(v_1)}{\left|p'_1(v_1)\right|} + \frac{f(v_2)}{\left|p'_2(v_2)\right|}$$

, where v_1, v_2 can be obtained through inversing the p-v function

$$v_1 = v_{mid} + c \cdot \log\left(\frac{p}{P_r - p}\right)$$

$$v_2 = v_{lim} + (\frac{1}{\alpha}\frac{P_r - p}{P_r})^{1/q}$$

The derivative of $p_{1,}\, p_2$ are

$$p'_1(v) = \frac{P_r}{c}\exp\left(\frac{v - v_{mid}}{c}\right)[1 + \exp\left(\frac{v - v_{mid}}{c}\right)]^{-2}$$

$$p'_2(v) = -2\alpha P_r(v - v_{lim})$$

Note that the probability output wind power has to be reckoned point-wise, for a certain value of power, firstly compute the corresponding v_1, v_2, then get the derivative value of $p_{1,}\, p_2$, the uncertainty of power is generated at last.

Following the steps above, a simulative wind farm can be produced as addressed below. Assume the rated output of this wind farm is 40MW. The scale parameter $\lambda = 13$ and the shape parameter $k = 2.1$ in the weibull distribution function. The wind speed varies from 0m/s to 40m/s with the step of 0.1m/s. Then using MATLAB to get the pdf of wind speed, the figure of this distribution function is shown in figure 4.

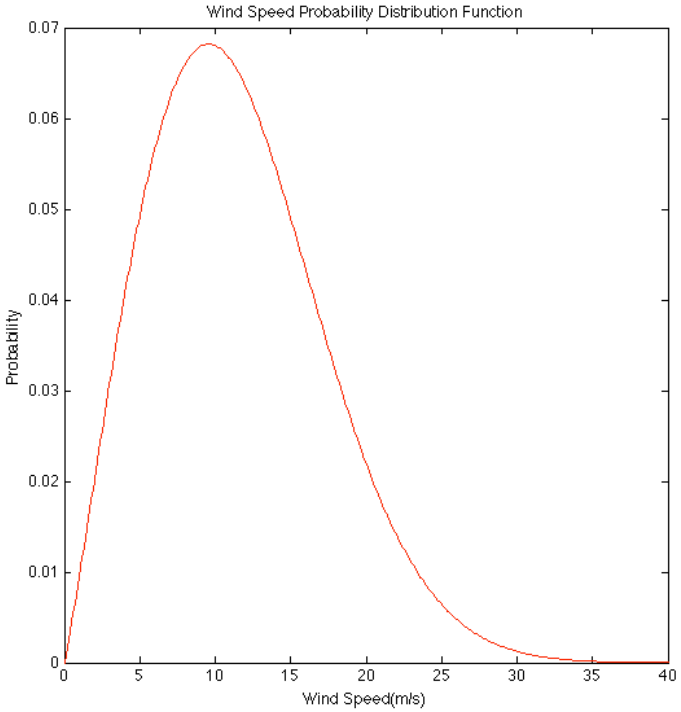

Figure 4. Wind Speed Probability Distribution Function (pdf)

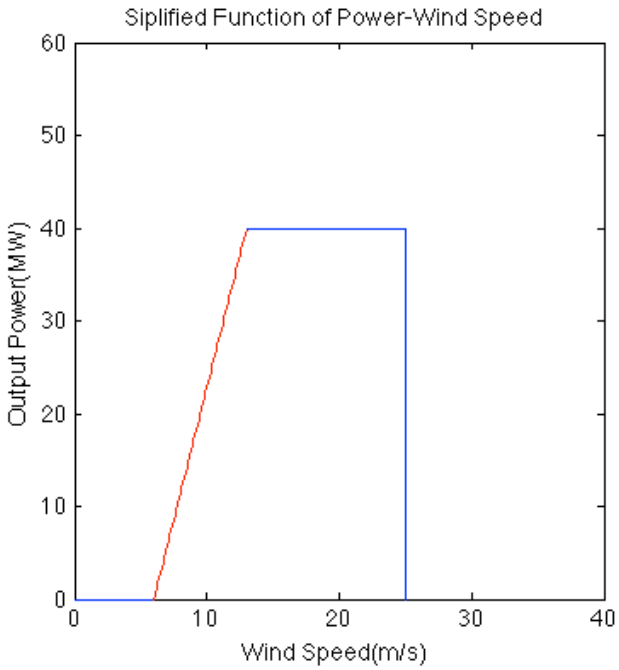

Figure 5. Simplified Output Power-Wind Speed Function

Observed the wind farm output power function with of wind speed described above, it's easy to find out that the period from cut-in wind speed to the rated wind speed can be simplified as a linear function. Assume the cut-in speed is 6m/s, rated wind speed is 13m/s and the cut-out speed is 25m/s. The simplified relationship between output power and wind speed is shown in Figure 5.

Then doing the integration of the wind speed pdf, first we can find out the probability of $P_{0,}$ which denotes the probability when there is, no output power

$$P_0 = P(v \leq 6) + P(v > 25) = 0.1789 + 0.0193 = 0.1982$$

Then the probability of rated power P_r, which is calculated by integral the pdf from 13m/s to 25m/s, is

$$P_r = P(13 \leq v \leq 25) = 0.3486$$

The practical wind turbine generally designed to output constant power in a small range of wind speed. Based on this practical and the linear feature of the power-wind speed function, we can divide the wind speed from 6m/s to 13m/s into 7 intervals，evenly; each of those corresponds to a certain value of output power. Each intervals of wind speed has a constant increment of 5MW output power. Then it's quite straightforward to calculate

the probability of each value of output power by integration. The probability calculating results are shown in Table 3.

Table 3. Probabilities of Each Level of Output Power

Output Power/MW	0	5	10	15	20	25	30	35	40
Probability	0.1982	0.0596	0.0643	0.0671	0.0681	0.0674	0.0651	0.0616	0.3486

When the VSA incorporating the wind power penetration, the probabilities of output are the probabilities of loading margins under different levels of wind power penetrations.

2.4 Brief Summary

1) The fundamental concepts of P-V curve and P-Q region was introduced and how to utilize in VSA was addressed in detail.
2) Based on the methodology to form those curves, under the circumstance of MATLAB, pseudo codes were listed in 2.2 to describe how to plot P-V curve and P-Q region in the test system.
3) Investigated the computational framework of wind power probability, a simplified way to calculate the probability of wind farm output was applied to an assumed wind farm.

CHAPTER 3 - SIMULATION RESULTS WITHOUT WIND POWER PENETRATION

In this chapter, conventional P-V curves of IEEE 30-bus system are generated utilizing MATPOWER. The load margins corresponding to voltage=0.95, power factor=0.8 both for real power and reactive power are calculated utilizing P-V curves and P-Q regions, respectively. The results strongly verify the availability of P-Q regions applied to assessing the voltage stable margins. Also, P-V curves are used to predict the voltage collapse point and assess the corresponding critical load margins.

3.1 Introduction of IEEE 30-bus test system

The roles of P-V curve and P-Q region in voltage stability assessment were investigated by using the IEEE 30-bus test system. Figure 6 shows the one-line diagram of this system. Bus 1, bus 2, bus 13, bus 22, bus 23 and bus 27 are connected with a generator respectively. Bus 1 is set as the swing bus while the others are considered as PV buses. The rest buses of this system are PQ buses.

The branch data of this system is demonstrated in Table 4. The parameters of the transmission lines can be used to calculate the losses on

the transmission lines so that by comparing the r, x, and b values, one can identify the weak bus incorporating the load condition on the buses.

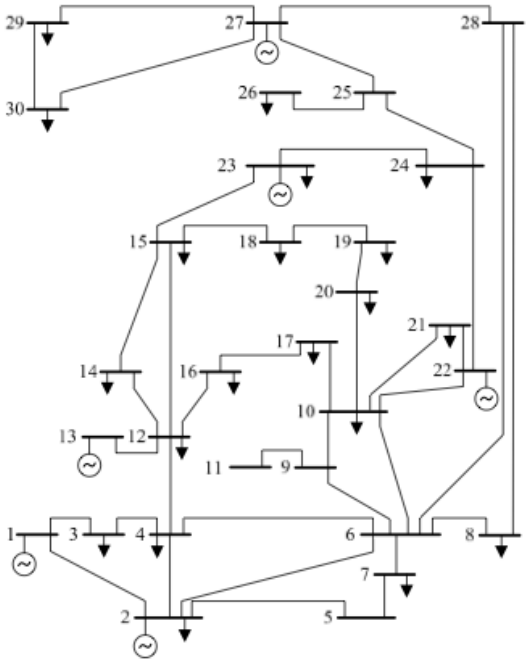

Figure 6. Single Line Diagram of IEEE 30-bus Test System

Table 4. Branch Data of the IEEE 30-Bus System

Branch no.	From bus	To bus	r (p.u.)	x (p.u.)	b (p.u.)
1	1	2	0.02	0.06	0.03
2	1	3	0.05	0.19	0.02
3	2	4	0.06	0.17	0.02
4	3	4	0.01	0.04	0
5	2	5	0.05	0.2	0.02
6	2	6	0.06	0.18	0.02
7	4	6	0.01	0.04	0
8	5	7	0.05	0.12	0.01
9	6	7	0.03	0.08	0.01
10	6	8	0.01	0.04	0
11	6	9	0	0.21	0
12	6	10	0	0.56	0
13	9	11	0	0.21	0
14	9	10	0	0.11	0

15	4	12	0	0.26	0
16	12	16	0.09	0.2	0
17	14	15	0.22	0.2	0
18	16	17	0.08	0.19	0
19	15	18	0.11	0.22	0
20	18	19	0.06	0.13	0
21	19	20	0.03	0.07	0
22	10	20	0.09	0.21	0
23	10	17	0.03	0.07	0
24	12	13	0	0.14	0
25	12	14	0.12	0.26	0
26	12	15	0.07	0.13	0
27	10	21	0.03	0.07	0
28	10	22	0.07	0.15	0
29	21	22	0.01	0.02	0
30	15	23	0.1	0.2	0
31	22	24	0.12	0.18	0
32	23	24	0.13	0.27	0
33	24	25	0.19	0.33	0
34	25	26	0.25	0.38	0
35	25	27	0.11	0.21	0
36	28	27	0	0.4	0
37	27	29	0.22	0.42	0
38	27	30	0.32	0.6	0
39	29	30	0.24	0.45	0
40	8	28	0.06	0.2	0.02
41	6	28	0.02	0.06	0.01

3.2 P-V Curves

P-V curves indicate the relationship between the growing load and the progressively descending bus voltage. It’s very intuitionistic to identify the weakest bus on the P-V curve diagram. What’s more, the real power margin for a fixed value of critical bus voltage can be easily obtained if the operating point is given.

For it's a time-consuming process and unnecessary if all the buses' P-V curves are supposed to be drawn, only considering those buses those have higher risk of voltage instability can prompt a more efficient method without losing accuracy. Selected in this way, buses connected directly to the swing bus and PV buses won't be considered into this range. Buses 3, 4, 5, 6, 10, 12, 15, 21, 24, 25, 28, 29, 30 are connected to the slack bus or PV bus, so only the P-V curves of buses 7, 8, 9, 11, 14, 16, 17, 18, 19, 26 are shown in figure 7.

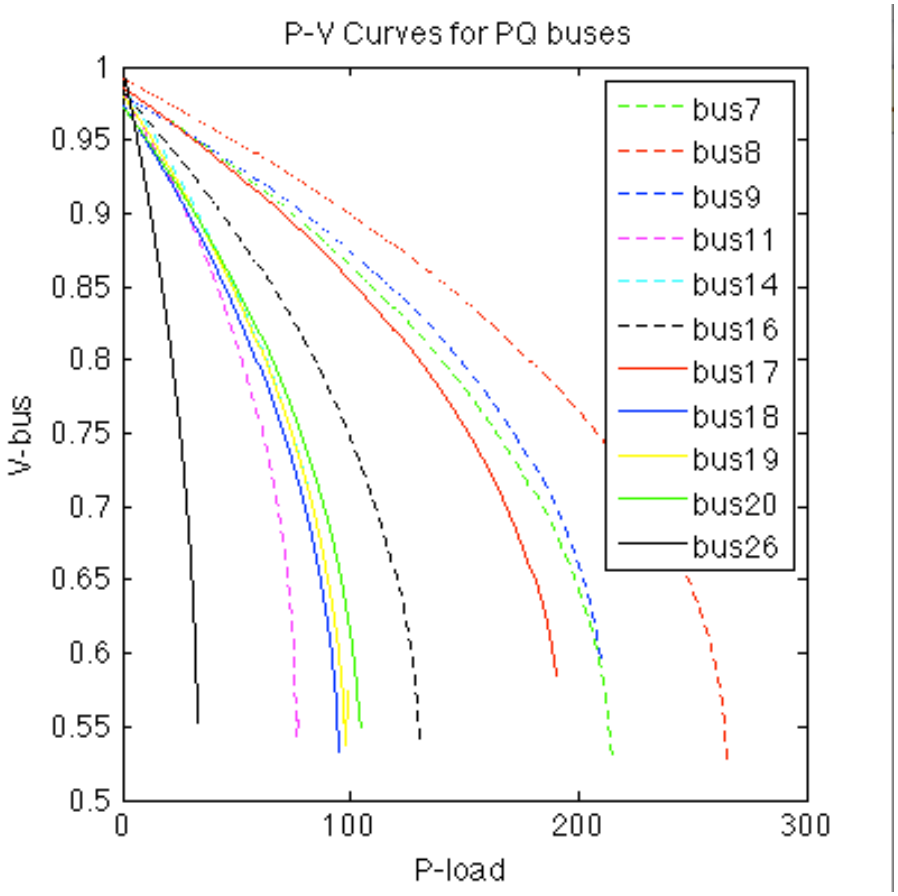

Figure 7. P-V curves of different PQ buses

P-V curve is supposed to be a “nose” curve that is divided by the “nose point” into two parts. The upper one has a degrading rate while the corresponding lower part is ascending. The “nose point” stands for the voltage collapse because after this point, bus voltage will continue descending even if the loading is shedding. The power flow solving method adopted in MATPOWER can’t reach the points after the “nose” due to the convergence problem. However, since the purpose is to find out the margin of voltage instability, the lower part of this curve seems not so important.

It’s not difficult to tell the weakest bus is bus 26 for the fastest voltage dropping regarding to the picking-up load, and the load margins arranged from small to big are bus 26 < bus 11 < bus 18 < bus 19 ≈ bus 14 < bus 20 < bus 16 < bus 17 < bus 7 < bus 9 < bus 8. The load power factor on each bus is fixed to 0.8. Observing the distance between the PQ buses and its nearest PV buses can get the intuitive judgment of weakest bus. Theoretically, the weakest bus is fastest away from the power supplement; however, the losses on the transmission lines that are affected by the impedance of transmission lines should be considered when determining the weakest bus. Calculation can be complicated and inefficiency if all the factors are considered to get more precise result. So only by judging the numbers of buses between the objective bus and its nearest bus is not sufficient to lead to a right result. For

instance, the load margin of bus 19 is larger than that of bus 18, while there're one more bus between bus 19 and PV bus 22 compared to bus 18 to bus 22.

Every respective load has its corresponding bus voltage on each PQ bus if the rest system is considered unchangeable. Assume the voltage requirements on each bus are all 0.95, the margins of P load and Q load are demonstrated in Table 5. P_{load} is the original real power load on the PQ bus. The unit for P is MW, and for Q is Mvar.

Table 5. The Load Margin Corresponding to V=0.95 on Each Bus

Bus no.	P_{load}	Q_{load}	$P_{0.95}$	$Q_{0.95}$	P Margin	Q Margin
7	22.8	10.9	32.9397	24.7048	10.1397	13.8048
8	30	30	48.8399	36.63	18.8399	6.63
9	0	0	33.1529	24.8647	33.1529	24.8647
11	0	0	11.6589	8.7442	11.6589	8.7442
14	6.2	1.6	14.6562	10.9921	8.4562	9.3921
16	3.5	1.8	18.2611	13.6959	14.7611	11.8959
17	9	5.8	31.4150	23.5613	22.4150	17.7613
18	3.2	0.9	9.5797	7.1848	6.3579	6.2848
19	9.5	3.4	12.7119	9.5339	3.2119	6.1339
20	2.2	0.7	10.2910	7.7182	8.0910	7.0182
26	3.5	1.8	6.1079	4.5809	2.6079	2.3809

The voltage stability margin, which is taken as an index of voltage stability, is defined as the real power distance between the collapse point and initial operating point. As shown in Table 6, the sensitivity of each bus is well illustrated by presenting the collapse voltage margin.

Table 6. Voltage Stability Margins with Corresponding Collapse Points

Bus no.	P_{load}	Q_{load}	Critical Voltage	$P_{critical}$	$Q_{critical}$	Collapse P Margin	Collapse Q Margin
7	22.8	10.9	0.5269	215	161.25	192.2	150.35
8	30	30	0.5290	265	198.75	235	168.75
9	0	0	0.5934	210	157.5	210	157.5
11	0	0	0.5553	77	57.75	77	57.75
14	6.2	1.6	0.5684	97	72.75	90.8	71.15
16	3.5	1.8	0.5389	130	97.5	126.5	95.7
17	9	5.8	0.5844	190	142.5	181	136.7
18	3.2	0.9	0.5331	95	71.25	91.8	70.35
19	9.5	3.4	0.5744	99	74.25	89.5	70.85
20	2.2	0.7	0.5499	105	78.75	102.8	104.3
26	3.5	1.8	0.5531	33	24.75	29.5	22.95

3.3 P-Q Region

P-Q region is used to determine the active load margin and reactive load margin to avoid critical voltage. For fixed bus voltage magnitude, the limit amounts of P and Q are computed by solving power flow utilizing MATPOWER. According to the concept of PV bus, the voltage magnitude is fixed on such buses and the real power generated on PV buses is specified. However, due to the limitation of generators, the generated or observed Q must within a certain range. If demand of Q beyond the limit, the PV bus can no longer keep its specified voltage magnitude and then can be treated as PQ bus. Using P-Q region to analyze a security of a PV bus is reasonable owing to its physical properties.

In order to get a better comparison with results got by using P-V curves, the P-Q regions for PV buses and PQ buses are illustrated respectively. For the default requirement of voltage magnitude on each PV bus, the P-Q regions are demonstrated in Figure 8. Note that the reactive power has negative value on each bus, which means that this bus can consume negative reactive load.

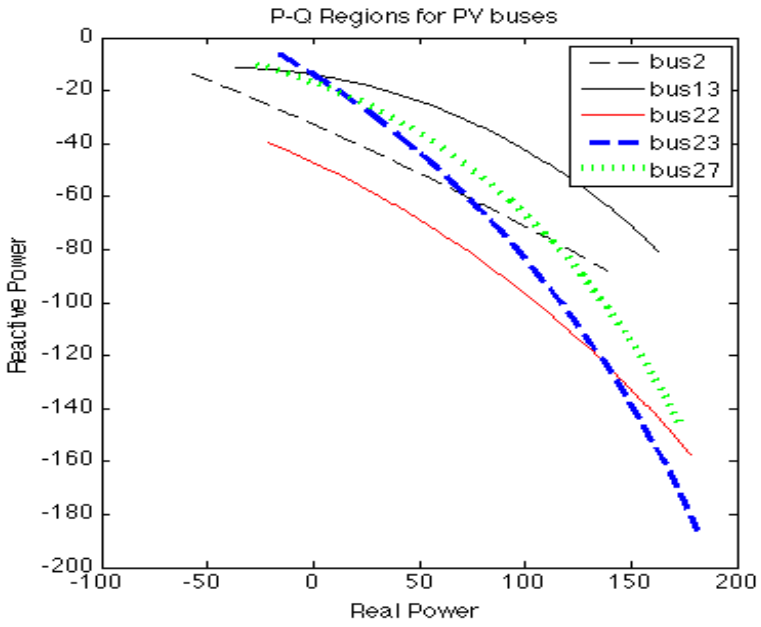

Figure 8. P-Q Regions for PV buses 2, 13, 22, 23, 27

Applying the little trick to PQ buses, which are considered as PV buses, we can get the P-Q regions for bus 7, 8, 9, 11, 14, 16, 17, 18, 19, 20, 26 when the voltages on each bus are all set to 0.95 as shown in Figure 9.

Similar conclusions can be drawn from P-Q regions in contrast to P-V curves for each bus. It's intuitive to identify the weakest bus that has the

smallest region. As long as the power factor is known, the P, Q margins for a certain voltage can be calculated using the method addressed in chapter 2.3. Utilizing P-Q regions, the calculated P, Q margins of each selected PQ buses corresponding to V=0.95 are shown in Table 7. The error compared to results got by P-V curves are also listed below. The unit for P is MW, and for Q is Mvar.

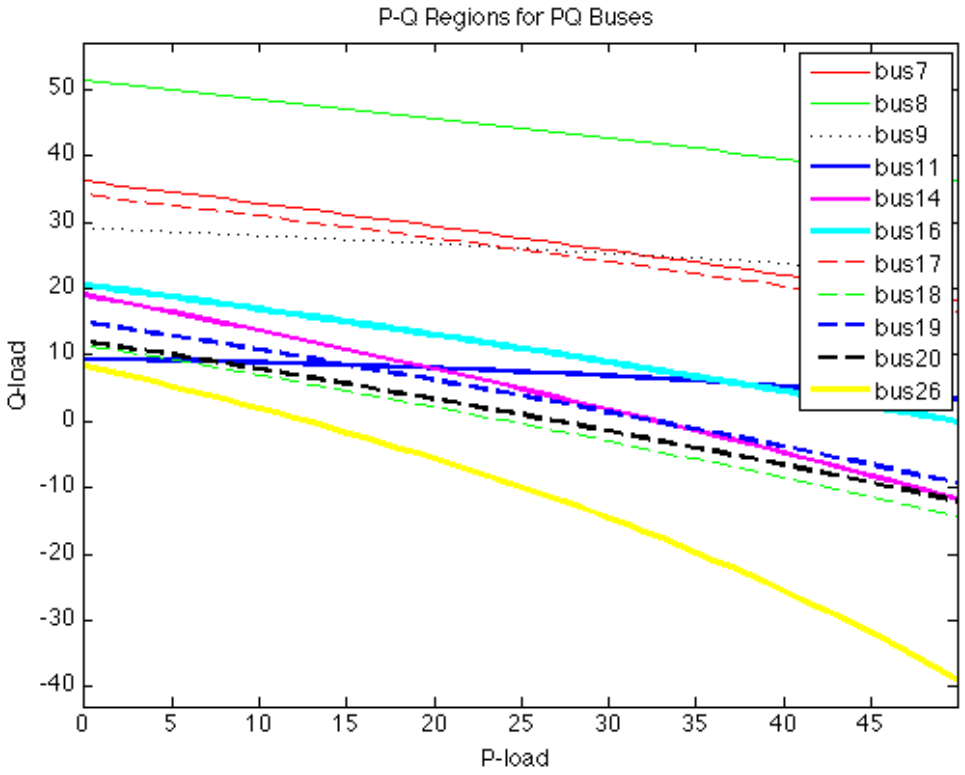

Figure 9. P-Q Regions for PQ buses 6, 7, 8, 9, 11, 14, 16, 17, 18, 19, 20, 26

The small errors of P, Q margins calculated by utilizing P-Q regions give a strong proof to the availability of P-Q regions in applying to the VSA. Using P-Q regions, it's easier to get the P, Q margins with distinct power factors of load, while for P-V curve, a family of curves must be generated in

order to meet the requirement of power factor, which is a quite time-consuming progress. However, P-V curve are of more practical meaning when forecasting the voltage collapse point since the voltage inability isn't known prior to generating the P-Q boundary.

Table 7. V=0.95, PF=0.8, Load Margins and Errors

Bus no.	$P_{0.95}$	$Q_{0.95}$	P Margin	Q Margin	Error P	Error Q
7	32.99	24.74	10.19	13.84	0.496%	0.255%
8	48.77	36.57	18.77	6.57	-0.371%	-0.904%
9	33.16	24.87	33.16	24.87	0.021%	0.021%
11	11.66	8.745	11.66	8.74	0.009%	0.009%
14	14.66	10.99	8.46	9.39	0.045%	0.022%
16	18.27	13.7	14.77	11.9	0.06%	0.034%
17	31.4	23.55	22.4	17.75	-0.067%	-0.064%
18	9.586	7.189	6.386	6.289	0.441%	0.067%
19	12.72	9.541	3.22	6.141	0.252%	0.012%
20	10.3	7.721	8.1	7.021	0.11%	0.04%
26	6.12	4.59	2.62	2.29	0.463%	-3.81%

In the method of calculating the margin from the P-Q region, the point corresponding to the 0.95 voltage magnitude that represents the margins for P and Q is got by finding out the intersection of the line of power factor 0.8 and the P-Q boundary curve. However, the P-Q boundary curve is plotted using data got from load flow calculation. Therefore, to get the intersection point, the equation for the curve is needed using method of curve fitting. By solving the equation set of the fitting curve and the line of power factor, the intersection point can be calculated. In these approximate processes, the error can't be avoided. Then, the conclusion can be drawn as the P-Q region

is accurate to assess the real power and reactive power region and is more convenient compared to P-V curve.

3.4 Brief Summary

The P-V curves of selected PQ buses in the IEEE 30-bus system were plotted and both the loading margins corresponding to 0.95 bus voltage and the collapse margins are calculated.

Both the P-Q regions for PV buses and PQ buses were plotted and loading margins when bus voltage equals to 0.95 was calculated using P-Q regions. The results compared to those responsible to P-V curves showed a strong proof to verify the feasibility of using P-Q region to assess voltage stability margin.

CHAPTER 4 VSA INCORPORATING WIND POWER

Now that P-Q region, essentially speaking, represents the relationship between real power and reactive power affordable by the bus when the voltage requirement is given. The application of P-Q region on determining the proper bus to place wind is proposed in this chapter. Then the VSA incorporating wind power penetration will consider the probability of this variable energy [20].

4.1 P-Q Regions Used to Determine the Safe Operating Region of Wind Farm

Verified the validity of P-Q regions in assessing voltage stable margins, based on the analysis of properties lies behind the P-Q region, a novel method to determine the bus to be connected to the wind farm is proposed utilizing the P-Q region.

Since P-V curves can provide accurate information to find out the weaker buses in one system, then those buses can be chosen as candidate buses to place wind farm in order to improve their ability to maintain the voltage stability. Therefore, bus 26, 11, 18, 19 are selected as the candidate buses in IEEE 30-bus system. The voltage stable region use to determine the wind power penetration is formed by generating the P-Q region for each bus as shown in Figure 10. The x-axis represents the generated real power and

the y-axis is the corresponding reactive power in order to keep the set voltage magnitude. The safe operating bus voltage range is assumed from 0.95 to 1.05 and the rated output real power is 40MW. The region between two P-Q boundaries is the safe operating region for wind power.

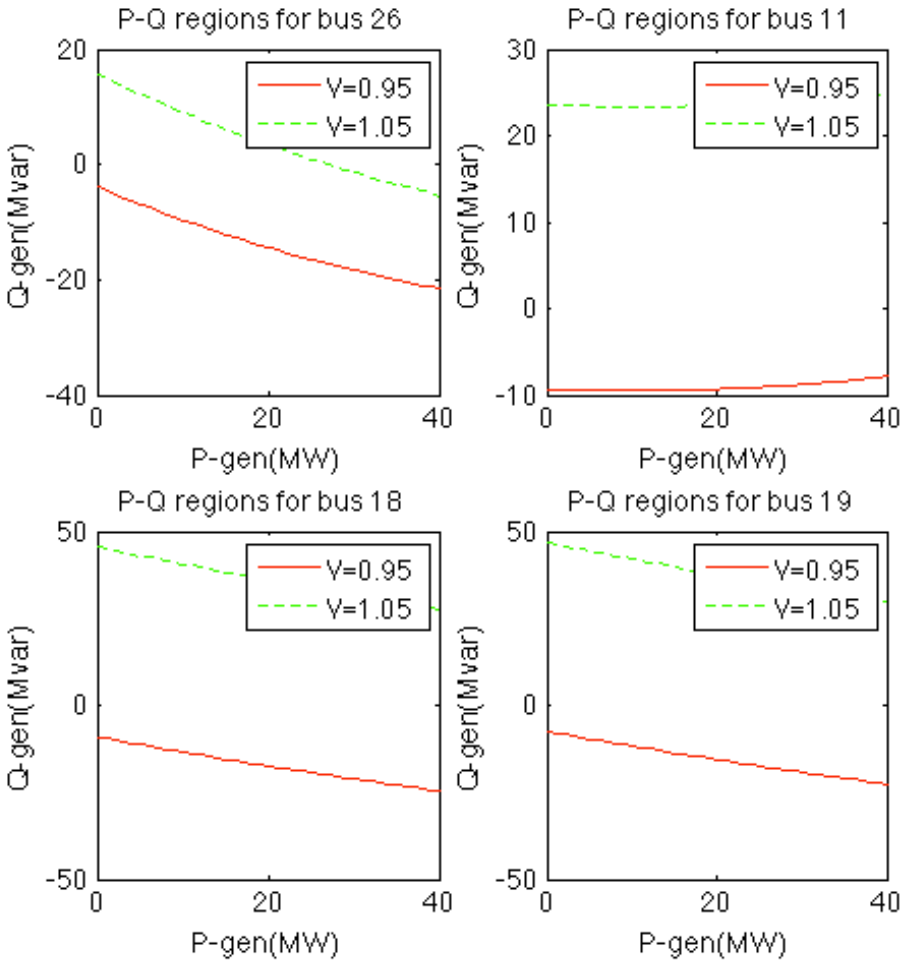

Figure 10. P-Q Regions for Candidate Buses

Although bus 26 is the weakest bus in this system, its P-Q region is relatively small compared to the other three. Bus 18 and bus 19 have the close range of safe regions, however, considering bus 18 is weaker

illustrated by P-V curves, we can choose bus 18 as the objective bus to place wind farm.

However, the safe region for operating wind power can't be just determined by this P-Q region. The limit of reactive power can give a tight constraint to this region. There are a number of ways to state to the requirement of reactive power control. The simplest is the fixed power factor. According to Federal Energy Regulatory Commission (FERC) mandated ± 0.95 power factor requirement, the safe operating region of bus 26 should be modified as illustrated in Figure 11.

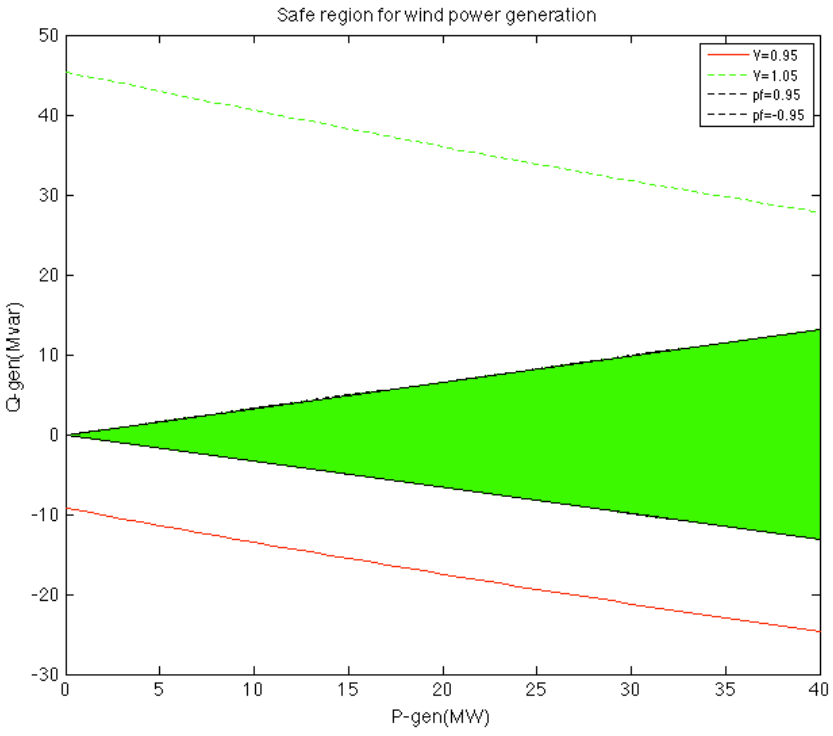

Figure 11. Safe Operating Region of Reactive Power Considering Q Constraints

The highlighted green zone is the safe region for wind farm operation in order to meet both the voltage requirement and the Q constraints. This safe operating region demonstrates the range of reactive power capability when the real power output increases from 0 MW to rated 40MW.

In practical operation of power system, the load condition can be approximately forecasted using the historical data. If the load condition is known in the future time period, the minimum output real power of wind farm could be predicted using the safe operating region. Figure 12 is an instance; the loading conditions on all the buses are set to three times of the base case.

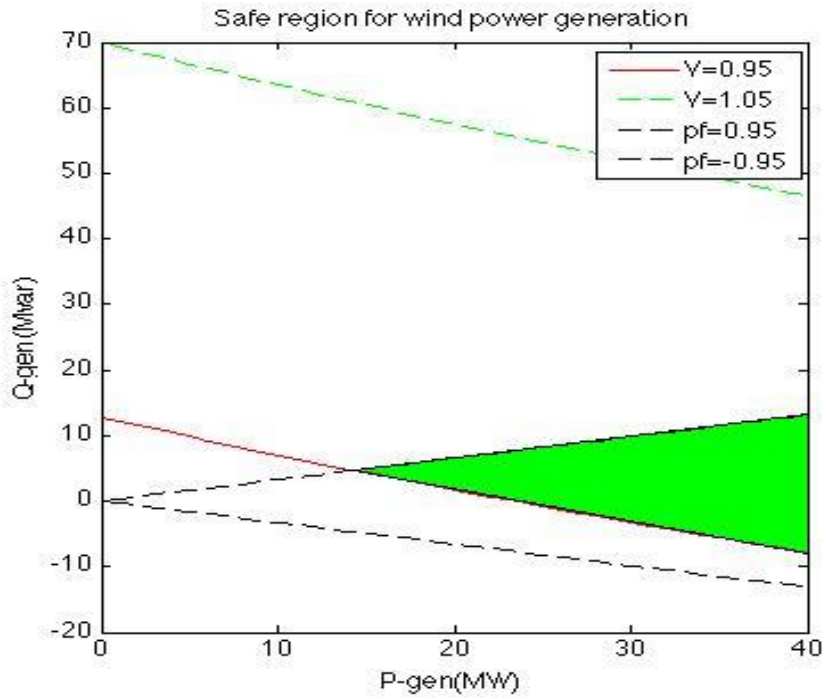

Figure 12. Safe Operating Region of Reactive Power, Total Loads Times 3

The intersection of lower boundary of P-Q region and the line corresponding to 0.95 power factor determines the minimum real power penetration of the wind farm. In this case, when the P load of the whole system increases to three times of the original case, the minimum output real power of the wind farm is 14.285MW. For a wind farm, we can evaluate the probability when the output power is no less than 14.285MW based on the distribution function of wind speed and the output power function of wind speed.

4.2 P-Q Region incorporating Wind Power

Bus 18 is chosen as the bus to place wind farm. Assume the rated output real power is 40MW, and then penetrations from 0MW to 40MW with the step of 10MW are incorporated when generating the P-Q regions for those critical buses with spot load. Figure 13 shows the impact of wind penetrations on bus 19, 20, 14 and 26.

The results show that the impact of wind penetration on the P-Q regions depends on the distance between the critical bus and the wind farm. The longer the distance is, the slighter the impact is. Therefore, the research of P-Q region incorporating wind penetration focuses on those buses who are close to the wind farm and have the spot load at the same time.

The conclusion that the P-Q region extends with the increasing penetration of wind power and consequently enlarge the P, Q margins of critical load bus. That can also explain why the wind farm is placed at or near the weak bus in the power system.

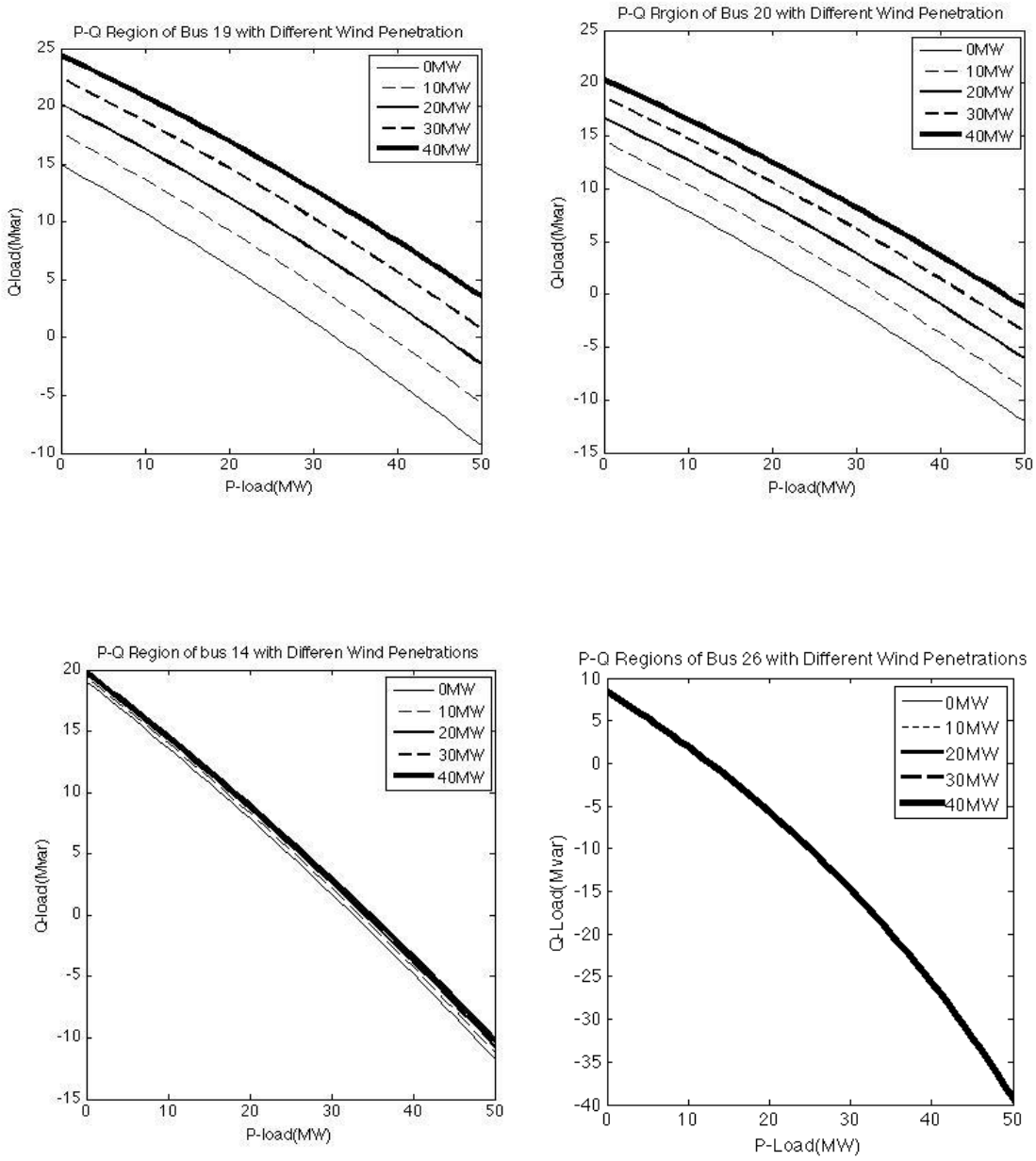

Figure 13. P-Q Regions of Critical Buses around the Wind Farm

4.3 VSA Incorporating Wind Penetration

The import of wind power to a power system is aim at reducing the cost of fossil fuels and therefore facilitates environment. In this part, 40 MW rated wind farm is assumed to be placed at bus 18 based on the analysis in 4.1. Accordingly, we may want to reduce 40MW electrical energy production from other PV buses. Assume the each generator on bus 13, 22, 23, 27 will reduce 10MW generation respectively. Then penetrate wind power on bus 18 from 0MW to 40MW with the step of 5MW. Since the effect of the variability of wind power is most obvious on bus 19, it is chosen as the critical bus to analyze its P-Q region and calculate its loading margins. The P-Q regions of bus 19 with different levels of wind power penetrations are shown in figure 14.

For each P, Q margins, there's a corresponding probability decided by the probability of the wind power penetration at this moment. Then the expected loading margin can be calculated by applying the statistics theory as illustrated in table 8.

Compared to the results got in 3.3 without wind power penetration, both the P margin and the Q margin enlarge a lot. For case 2, the generators of bus 13 no longer supply any real power to this system. Then the corresponding P-Q regions of bus 19 are demonstrated in figure 15.

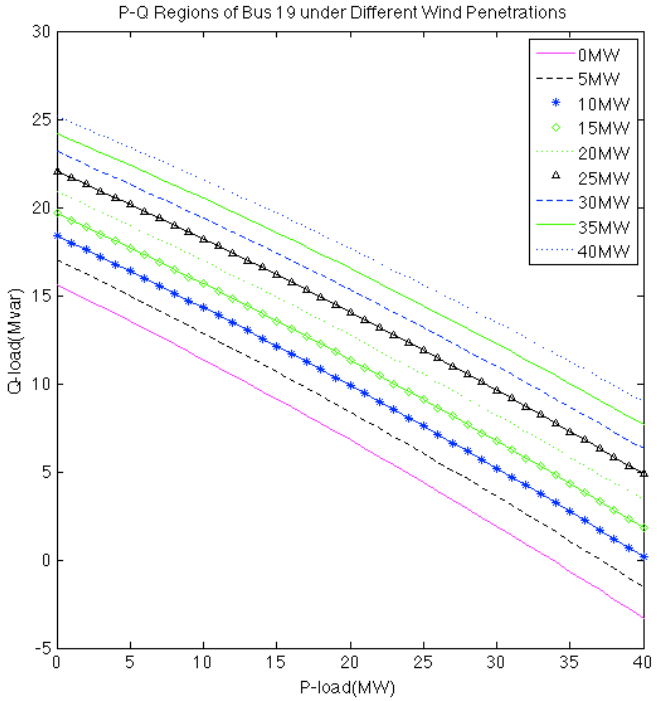

Figure 14. P-Q Regions of Bus 19 under Different Wind Power Penetrations

Table 8. Probabilities and Expected P, Q Margins for Bus 19

Wind Penetration	ΔP(MW)	ΔQ(Mvar)	Probability (p)	$\Delta P \times p$	$\Delta Q \times p$
0MW	3.7	6.497	0.1982	0.7333	1.2877
5MW	4.89	7.47	0.0596	0.2914	0.4452
10MW	6.25	8.41	0.0643	0.4019	0.5408
15MW	7.48	9.34	0.0671	0.5019	0.6267
20MW	8.66	10.22	0.0681	0.5897	0.6960
25MW	9.76	11.07	0.0674	0.6578	0.7461
30MW	10.88	11.88	0.0651	0.7083	0.7734
35MW	11.92	12.67	0.0616	0.7343	0.7805
40MW	12.93	13.42	0.3486	4.5074	4.6872
Expected ΔP(MW)		9.126	Expected ΔQ(Mvar)		10.5836

It's obvious the P-Q regions of bus 19 changes from the figure when the reduction of generation spreading on each PV buses. To illustrate the

results more clearly, P, Q margins and their expected values are still calculated as shown in Table 9.

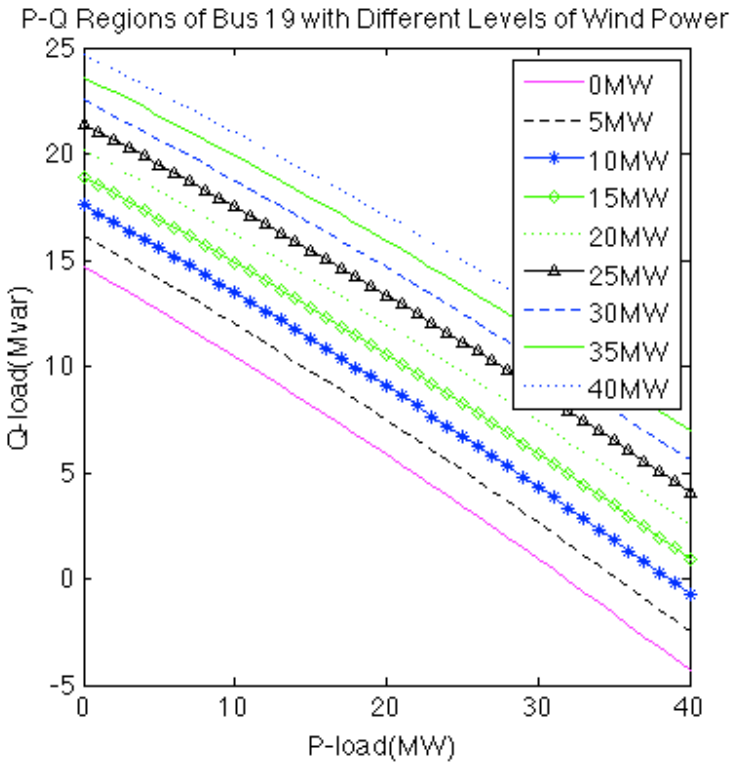

Figure 15. P-Q Regions of Bus 19 with 0MW Generation on Bus 13

Table 9. Probabilities and Expected P, Q Margins for Bus 19 with 0MW Generation on Bus 13

Wind Penetration	ΔP(MW)	ΔQ(Mvar)	Probability (p)	$\Delta P \times p$	$\Delta Q \times p$
0MW	2.96	5.943	0.1982	0.5867	1.1779
5MW	4.26	6.92	0.0596	0.2539	0.4124
10MW	5.53	7.87	0.0643	0.3556	0.5003
15MW	6.77	8.8	0.0671	0.4543	0.5905
20MW	7.95	9.69	0.0681	0.5414	0.6599
25MW	9.09	10.54	0.0674	0.6127	0.7104
30MW	10.19	11.37	0.0651	0.6634	0.7402

35MW	11.25	12.16	0.0616	0.693	0.7491
40MW	12.26	12.92	0.3486	4.2738	4.5039
Expected Δ*P*(MW)		8.4348	Expected ΔQ(Mvar)		10.0446

The P, Q margins in this case shrink a bit compared to first case. However, they are still much larger than the original case without penetrations of wind power. Therefore, choosing a proper bus to place to wind farm can facilitate enlarging the voltage stability margin.

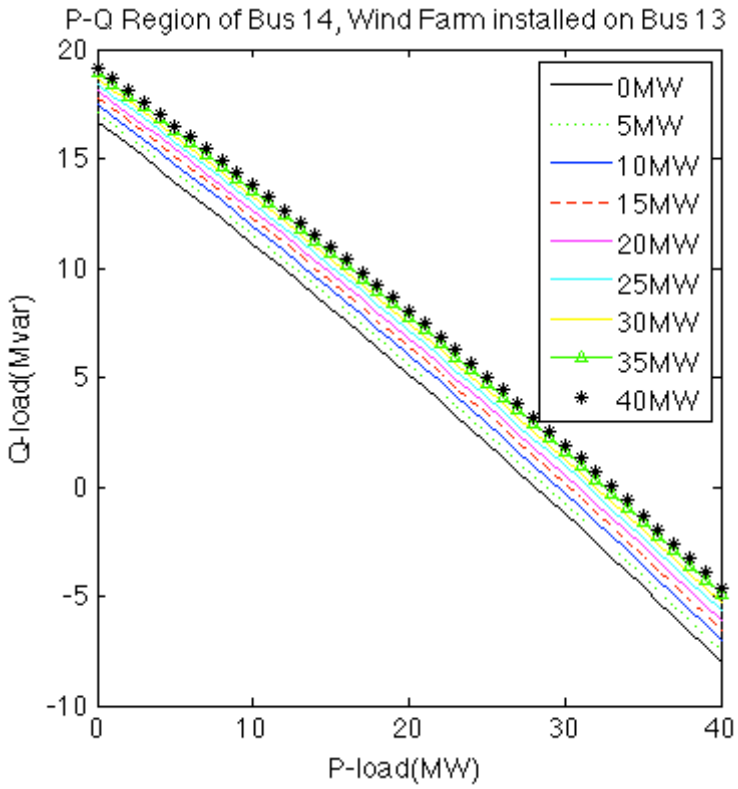

Figure 16 P-Q Region of Bus 14, Wind Farm Installed on Bus 13

Consider install the wind farm on PV bus 13, replacing the original conventional generator unit. Then the P-Q regions of bus 14 with different

levels of wind power penetrations are shown in figure 16. The corresponding expected loading margin is calculated in table 10.

Table 10. Probabilities and Expected P, Q Margins for Bus 14, Wind Farm Installed on Bus 13

Wind Penetration	ΔP(MW)	ΔQ(Mvar)	Probability（p）	$\Delta P \times p$	$\Delta Q \times p$
0MW	6.49	7.92	0.1982	1.2863	1.5697
5MW	6.82	8.169	0.0596	0.4065	0.4868
10MW	7.12	8.395	0.0643	0.4578	0.5398
15MW	7.41	8.61	0.0671	0.4972	0.5777
20MW	7.28	8.81	0.0681	0.4958	0.60
25MW	7.93	9.00	0.0674	0.5345	0.6066
30MW	8.16	9.17	0.0651	0.5312	0.5970
35MW	8.38	9.33	0.0616	0.5162	0.5747
40MW	8.57	9.48	0.3486	2.9875	3.3047
Expected ΔP(MW)		7.713	Expected ΔQ(Mvar)		8.857

The results shows that compared to the original case, in which the P margin is 8.46MWand the Q margin is 9.39Mvar, the expected loading margin is 91.2% and 94.3% of the original case, respectively.

4.4 Brief Summary

1) P-Q region was used to determine the best bus to place wind farm considering the reactive power constrains. This application can provide a reference of minimum output wind farm when the loading forecasting curve is known.

2) The simulation results show that only those close to the wind farm can be affected obviously by the variable nature of this energy.
3) The P-Q regions of bus 19 under different levels of wind power penetration were plotted in two cases. The expected loading margins in both cases are larger than the original case without wind power.
4) The expected loading margin calculated from the P-Q regions of bus 14 when the wind farm is installed on bus 13 to replace the original conventional generator unit show that this variable energy will cause smaller loading margin.

CHAPTER 5 CONCLUSIONS AND FUTURE WORK

5.1 Main Conclusions

Based on investigation of the methods of VSA, this dissertation addressed the theoretical analysis of the P-V curve and the P-Q region, plotted the P-V curve and the P-Q region utilizing MATPOWER, and proposed the applications of the P-Q regions when incorporating the wind power. The main conclusions can be drawn as follows.

1. Deeply investigated the theoretical basis of voltage instability; analyzed the relationship between real power load and bus voltage using deduced formulas of load flow equations; studied the novel method of using the P-Q region to assess system voltage stability; proposed to plot both the P-V curve and the P-Q region utilizing the simulation tool MATPOWER. Although the P-V curve is a more feasible way to forecast the voltage collapse point, from a practical view of VSA, the loading margins corresponding to required bus voltage are of more interest. The P-Q is found to be a better option used in VSA since there's no need to generate a family of P-V curves in order to get the loading margins with distinct power factors under the requirement of a certain bus voltage magnitude.

2. Proposed a novel method which treats a PQ bus as a PV bus when plotting the P-Q region for the PQ bus. This method saved masses of load flow calculations with simulated the P-V curves and the P-Q regions of selected buses in IEEE 30-bus system. Then the loading margins calculated from the P-V curves and the P-Q regions were contrasted. The minute-error results showed a powerful proof of the feasibility of utilizing the P-Q region in VSA.
3. Applied the idea of VSA using the P-Q region, the best location for the wind farm in a power system can be determined by comparing the range of reactive power when the requirement of bus voltage is a certain interval. According to the bus sequence of voltage stability that is confirmed by P-V curves, bus 18 was chosen as the most proper spot to build a wind farm.
4. Another application of P-Q region is to assess the safe operating region for a wind farm under the reactive power constraint. This safe operating region can give the margin of reactive corresponding to each value of real power output. The result is meaningful due to the variable nature of wind energy. What's more, the forecasting loading curve is always known by the operators, which combines the safe

operating region of wind farm, can decide the minimum output of the wind farm in order to keep the bus voltage in a satisfying range.

5. A wind farm was modeled with weibull distribution. The calculated probabilities of the output power are incorporated into the P-Q regions that are plotted under different levels of wind power penetrations. The expected loading margins were calculated for two cases. The first case for reduction of 10MW real power generation on 4 PV buses, while the second one considered using wind farm to replace the generators on bus 13, which has the approximate generation of the rated power of the wind farm. The expected loading margins in the second case are smaller than the first case, which validates to the assumption that the schemes of replacing proper PV bus affects the loading margins. However, in both cases, the expected margins extend significantly in comparison to the original case. This result gave a satisfactory answer of choosing bus 18 to place the wind farm.
6. The expected P and Q loading margin of bus 14 when the wind farm is installed on bus 13 is 91.2% and 94.3% of original case respectively. This is reasonable because the wind farm cannot supply the rated power at all the time.

5.2 Future Work

The results of the research provide a theoretical foundation of various applications of P-Q region. The conclusions show the practical meaning of P-Q region utilizing in VSA and stability-related problems incorporating wind power. Particularly, the future work should be focused on these aspects.

1. A realistic systems should be investigated with the method of P-Q region to VSA;
2. Contingencies should be included into VSA utilizing P-Q region;
3. A more accurate method of calculating the probabilities of wind power should be considered in the VSA.
4. A design of Graphical User Interface (GUI) for the P-Q region should be developed, which can be a useful tool for the area of VSA applying to the wind power.

References

[1] Taylor, Carson W. *Power system voltage stability*. McGraw-Hill Companies, 1994.

[2] YIN, Yong-hua, et al. "Preliminary analysis of large scale blackout in interconnected North America power grid on august 14 and lessons to be drawn." *Power system technology* 10 (2003): 001.

[3] Kundur, Prabha. *Power system stability and control*. Tata McGraw-Hill Education, 1994.

[4] Kundur, Prabha, et al. "Definition and classification of power system stability IEEE/CIGRE joint task force on stability terms and definitions." *IEEE Transactions on Power Systems*19.3 (2004): 1387-1401.

[5] Gao, B., G. K. Morison, and P. Kundur. "Towards the development of a systematic approach for voltage stability assessment of large-scale power systems." *IEEE Transactions on Power Systems* 11.3 (1996): 1314-1324.

[6] Gao, Baofu, G. K. Morison, and Prabhashankar Kundur. "Voltage stability evaluation using modal analysis." *IEEE Transactions on Power Systems* 7.4 (1992): 1529-1542.

[7] Clark, H. K. "New challenge: voltage stability." *IEEE Power Engineering Review* (1990): 30-37.

[8] Gupta, R. K., et al. "Steady state voltage instability operations perspective." *IEEE Transactions on Power Systems* 5.4 (1990): 1345-1354.

[9] Yokoyama, Akihiko, Teruhisa Kumano, and Yasuji Sekine. "Static voltage stability index using multiple load-flow solutions." *Electrical Engineering in Japan* 111.3 (1991): 69-79.

[10] Tiranuchit, A., and R. J. Thomas. "A posturing strategy against voltage instabilities in electric power systems." *IEEE Transactions on Power Systems* 3.1 (1988): 87-93.

[11] Zhang, Yang, Sidharth Rajagopalan, and José Conto. "Practical Voltage Stability Analysis." *IEEE Power and Energy Society General Meeting* (2010):1-7.

[12] Chowdhury, Badrul H., and Carson W. Taylor. "Voltage stability analysis: VQ power flow simulation versus dynamic simulation." *IEEE Transactions on Power Systems* 15.4 (2000): 1354-1359.

[13] Haque, M. H. "Determination of steady-state voltage stability limit using PQ curve." *IEEE Power Engineering Review* 22.4 (2002): 71-72.

[14] Alonso, Mónica, and Hortensia Amarís. *Impact of Wind Farms in Power Systems.* Intech Company, 2011.

[15] Lu, Jin, Chih-Wen Liu, and James S. Thorp. "New methods for computing a saddle-node bifurcation point for voltage stability analysis." *IEEE Transactions on Power Systems* 10.2 (1995): 978-989.

[16] Sobierajski, M., and M. Fulczyk. "Use of pq curve with rectangular probability distribution of bus load in voltage stability study." *IEEE PES Power Systems Conference and Exposition* (2004):130-136.

[17] Glavic, Mevludin, et al. "See It Fast to Keep Calm: Real-Time Voltage Control Under Stressed Conditions." *IEEE Power and Energy Magazine* 10.4 (2012): 43-55.

[18] Dhople, Sairaj V., and Alejandro D. Domínguez-García. "A framework to determine the probability density function for the output power of wind farms." *IEEE North American Power Symposium (NAPS)* (2012):1-6.

[19] Vestas, "V90-1.8/2.0 MW data sheet," 2011. [Online]. Available: http://www.vestas.com

[20] El-Saadawi, M. M., et al. "Impact of wind farms on contingent power system voltage stability." *IEEE 12th International Middle-East Power System Conference* (2008):637-644.